International Research Journal of Engineering and Technology (IRJET) e-ISSN: 2395-0056
Volume: 06 Issue: 11 | Nov 2019 www.irjet.net p-ISSN: 2395-0072

AERODYNAMIC ANALYSIS ON A CAR TO REDUCE DRAG FORCE USING VERTEX GENERATOR

MRS CHAITANYA MAYEE M[1], YAMALA PRIYANKA[2]

[1]Assistant Professor, Dept. of Mechanical Engineering, S.V.P. Engineering College, Visakhapatnam.
[2]Dept. of Mechanical Engineering. S.V.P. Engineering College. Visakhapatnam.

ABSTRACT - *Now a days with an increase in competition, the vehicle aerodynamics plays an important role. Aerodynamics affects the performance of vehicle due to change in parameters such as lift and drag forces which play a significant role at high speed and fuel economy. With an improvement in computer technology, manufacturers are looking toward computational fluid dynamics instead of wind tunnel testing to reduce the testing time and cost. Our project main aim is to reduce aerodynamic drag coefficient by improving the design of a vehicle, which is possible by placing vertex generators at rear top of vehicle. It Makes the car safer and make it fuel efficient.*

KEYWORDS: *Vortex generators, Aerodynamics, Drag, Lift, Drag coefficient, Lift coefficient, CFD*

INTRODUCTION

Automotive aerodynamics is the study of the aerodynamics of road vehicles. Its main goals are reducing drag and wind noise, minimizing noise emission, and preventing undesired lift forces and other causes of aerodynamic instability at high speeds. Air is also considered a fluid in this case. For some classes of racing vehicles, it may also be important to produce down force to improve traction and thus cornering abilities.

Aerodynamics was first used to increase vehicle performance in race cars during the 1970s. Race car engineers realized that air flowing around the vehicle could be used to increase down force and reduce aerodynamic drag on the car. As fuel economy became a strong factor in road vehicle design, engineers soon realized that the methods of reducing aerodynamic drag on race cars could be transferred to road vehicles in order to improve fuel economy. To decrease the amount of drag created by a vehicle, automobile manufacturers began incorporating vehicle body designs that would allow the vehicle to be more streamlined. Methods of decreasing the drag coefficient of a vehicle include re-shaping the rear end, covering the underside of the vehicles, and reducing the amount of protrusions on the surface of the car. Imagine holding a large traffic cone outside of your car window while driving on a freeway at seventy-five miles per hour. You are given two options: either holds the cone so that the pointed end faces the same direction the car is moving, or so the pointed end faces away from the direction the car is moving. In which scenario would it be easier to hold the cone, given the effects of air resistance? While intuition may cause many to think that holding the pointed end of the cone forward is more effective, the opposite is actually true. This phenomenon is an example of aerodynamic drag, the concept that engineers use to design the car's shape and minimize the engine power needed to push the car forward. Optimizing the shape of a vehicle to reduce aerodynamic drag can allow vehicle designers to build cars with increased fuel economy. Little effort is needed to reveal the ever-increasing importance of fuel economy for production vehicles. Better automotive aerodynamics lead to a reduction in fuel consumption, helping drivers save money and lowering carbon dioxide emissions. One important consideration that modern vehicle engineers take into account while designing a car is aerodynamics. Aerodynamics is the study of both the motion of air and the forces created on an object moving through air. When an automobile is in motion, a large amount of air is displaced and must flow around the vehicle.

The auto industry has seen a continual increase in the level of global competition. The growth in the complexity of vehicle design and content has led to expensive and time - consuming development processes. The large cost and long gestation imply very significant risk for the automaker. At the same time, it is clear that technology will play an ever-increasing role as the basis of this global competition, requiring high quality products that are safe to use, and economical to design and manufacture. The climate has been favorable for the increasing use of Computer-Aided Engineering (CAE) tools for math-based analysis of candidate designs and product features.

LITERATURE REVIEW

Sneh Hetawal et al. [1] 2014

This article describes the design and CFD analysis of a Formula SAE car. A numerical study of a rear engine SAE race car is presented. The focus of the study is to investigate the aerodynamics characteristics of a SAE race car with front spoiler, without front spoiler and with

firewall vents. The aerodynamics study of the SAE car is made to reduce the drag force. The study was performed using the CFD package. The main goal of this study is to enhance the stability of the vehicle and reduce the drag. With this the track performance will be increased also the resistance of air to the vehicle gets reduced.

S.M. Rakibul Hassan et al. [2]2013

By study of this article we have observed 50 to 60% of total fuel energy is lost due to this aerodynamic force. This article is concentrated on different aspects analysis of aerodynamic drag of racing cars and different drag reduction techniques such as rear under body modification and exhaust gas redirection towards the rear separation zones. The drag can be reduced up to 22.13% by different rear under-body modifications and up to 9.5% by exhaust gas redirection towards the separated region at the rear of the car. It is also evident that if somehow the negative pressure area and its intensity at the rear of the car can be minimized, the separation pressure drag is subsequently reduced.

S.Y. Cheng et al.[3] 2012a

The influence of transient flows on vehicle stability was investigated by large eddy simulation. To consider the dynamic response of a vehicle to real-life transient aerodynamics, a dimensionless parameter that quantifies the amount of aerodynamic damping for vehicle subjects to pitching oscillation is proposed. Two vehicle models with different stability characteristics were created to verify the parameter. For idealized notchback models, under body has the highest contribution to the total aerodynamic damping, which was up to 69%. However, the difference between the aerodynamic damping of models with distinct A- and C-pillar configurations mainly depends on the trunk-deck contribution. Comparison between dynamically obtained Phase-averaged pitching moments with quasi-steady values shows totally different aerodynamic behaviors.

D.E. Aljure et al. [5] 2014

The aim of the present study is focused on the assessment of different LES models (e.g. VMS or SIGMA models), as well as to show their capabilities of capturing the large-scale turbulent flow structures in car-like bodies using relative coarse grids. In order to achieve these objectives, the flow around two model car geometries, the Ahmed and the Asmo cars, is simulated. These generic bluff bodies reproduce the basic fluid dynamics features of real cars. First, the flow over both geometries is studied and compared against experimental results to validate the numerical results. Then, different LES models are used to study the flow in detail and compare the structures found in both geometries.

Chien-Hsiung Tsai et al. [8] 2009

This study proposes an effective numerical model based on the Computational Fluid Dynamics (CFD) approach to obtain the flow structure around a passenger car with wing type rear spoiler. The topology of the test vehicle and grid system is constructed by a commercial package, ICEM/CFD. FLUENT is the CFD solver employed in this study. The wind effect on the aerodynamic behavior of a passenger car with and without a rear spoiler and endplate is numerically investigated in the present study. It is found that the installation of a spoiler with an appropriate angle of attack can reduce the aerodynamic lift coefficient.

INTRODUCTION TO COMPUTER AIDED MODELING

Throughout the history of our industrial society, many inventions have been patented and whole new technologies have evolved. Perhaps the single development that has impacted manufacturing more quickly and significantly than any previous technology is the digital computer. Computers are being used increasingly for both design and detailing of engineering components in the drawing office.

Computer-aided design (CAD) is defined as the application of computers and graphics software to aid or enhance the product design from conceptualization to documentation. CAD is most commonly associated with the use of an interactive computer graphics system, referred to as a CAD system. Computer-aided design systems are powerful tools and in the mechanical design and geometric modeling of products and components.

CAD/CAM SOFTWARE:

Software allows the human user to turn a hardware configuration into a powerful design and manufacturing system. CAD/CAM software falls into two broad categories,2-D and 3-D, based on the number of dimensions are called 2-D representations of 3-D objects is inherently confusing. Equally problem has been the inability of manufacturing personnel to properly read and interpret complicated 2-D representations of objects. 3-D software permits the parts to be viewed with the 3-D planes-height, width, and depth-visible. The trend in CAD/CAM is toward 3-D representation of graphic images. Such representation approximates the actual shape and appearance of the object to be produced; therefore, they are easier to read and understand.

Initially, CATIA name is an abbreviation for Computer Aided Three-dimensional Interactive Application the French Dassault Systems is the parent company and IBM participates in the software and marketing, and CATIA is

invades broad industrial sectors, and has been explained in the previous post position of CATIA between 3d modelling software programs A Window will be opened and there are types of design.

From the above tools we are firstly going to use the datum tool. In datum tool we are going to choose sketch.

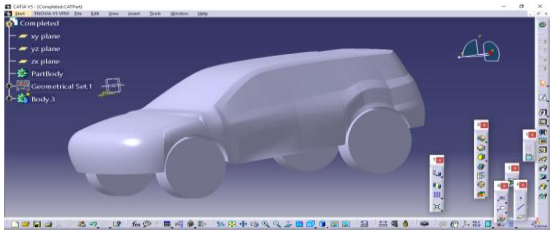

Fig: 4.1 full car model without VG

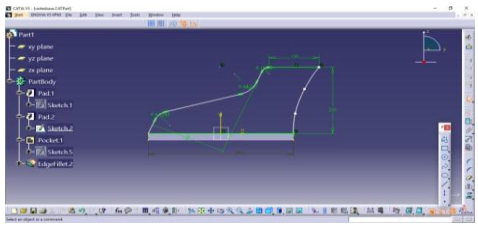

Fig: 4.2 sketch view of vertex generator model1

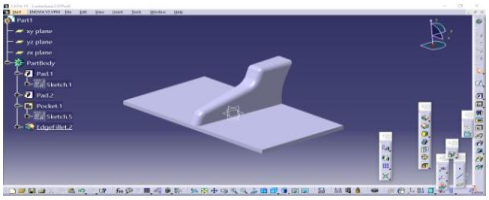

Fig: 4.3 vertex generator model1

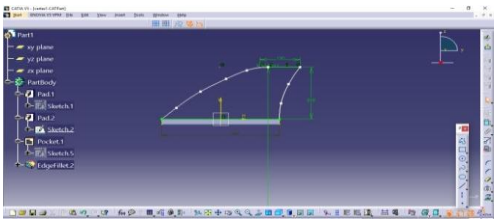

Fig: 4.5 sketch view of vertex generator model 2

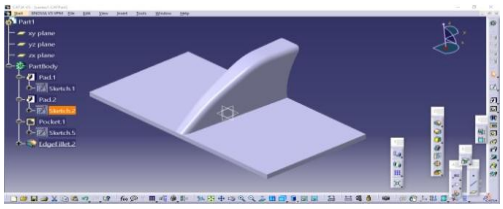

Fig: 4.6 vertex generator model 2

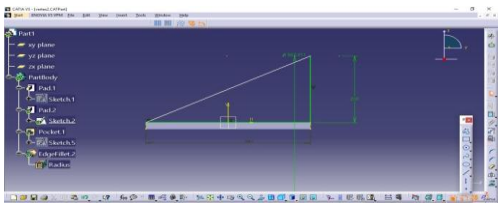

Fig: 4.8 sketch view of vertex generator model 3

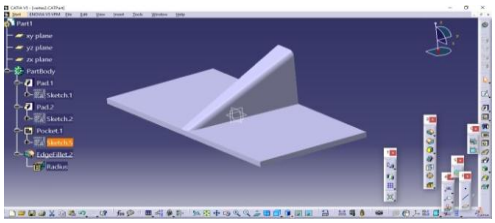

Fig: 4.9 vertex generator model 3

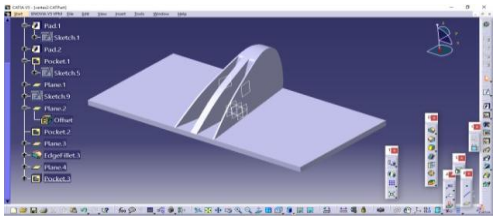

Fig: 4.11 vertex generator model 4

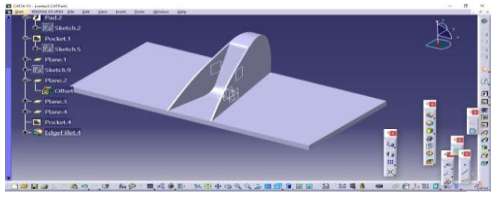

Fig: 4.11 vertex generator model 5

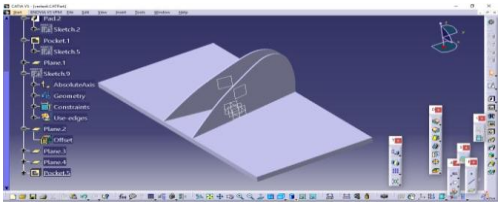

Fig: 4.15 vertex generator model 6

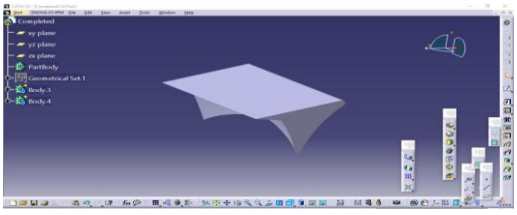

Fig: 4.17 vertex generator model 7

COMPUTATIONAL FLUID DYNAMICS

Computational Fluid Dynamics (CFD) is the science of predicting fluid flow, heat transfer, mass transfer, chemical reaction (e.g., combustion), and related phenomena by solving the mathematical equations that govern these processes using a numerical algorithm on a computer. The technique is very powerful and spans a wide range of industrial and non-industrial application areas.

CONTINUITY EQUATION:

The equation based on the principle of conservation of mass is called continuity equation. The conservation of mass law applied to a fluid passing through an infinitesimal, fixed control volume yields the following equation of continuity,

$$\frac{\partial \rho}{\partial t}+\frac{\partial(\rho u)}{\partial x}+\frac{\partial(\rho v)}{\partial y}+\frac{\partial(\rho w)}{\partial z}=0$$

$$\frac{\partial \rho}{\partial t}+\nabla.(\rho V)=0$$

Where 'ρ' is the fluid density, 'V' is the fluid velocity. For an incompressible flow, the density of each fluid element remains constant.

5.3 MOMENTUM EQUATIONS:

The equations based on the laws of conservation of momentum or on the principle of momentum, states that, the net force acting on fluid mass is equal to the change in momentum of flow per unit time in that direction. The Navier-Stokes equations in conservative form

$$\frac{\partial(\rho u)}{\partial t}+\frac{\partial(\rho u^2)}{\partial x}+\frac{\partial(\rho uv)}{\partial y}+\frac{\partial(\rho uw)}{\partial z}=-\frac{\partial p}{\partial x}+\frac{\partial \tau_{xx}}{\partial x}+\frac{\partial \tau_{yx}}{\partial y}+\frac{\partial \tau_{zx}}{\partial z}+\rho f_x$$

$$\frac{\partial(\rho v)}{\partial t}+\frac{\partial(\rho uv)}{\partial x}+\frac{\partial(\rho v^2)}{\partial y}+\frac{\partial(\rho vw)}{\partial z}=-\frac{\partial p}{\partial y}+\frac{\partial \tau_{xy}}{\partial x}+\frac{\partial \tau_{yy}}{\partial y}+\frac{\partial \tau_{zy}}{\partial z}+\rho f_y$$

$$\frac{\partial(\rho w)}{\partial t}+\frac{\partial(\rho uw)}{\partial x}+\frac{\partial(\rho vw)}{\partial y}+\frac{\partial(\rho w^2)}{\partial z}=-\frac{\partial p}{\partial z}+\frac{\partial \tau_{xz}}{\partial x}+\frac{\partial \tau_{yz}}{\partial y}+\frac{\partial \tau_{zz}}{\partial z}+\rho f_z$$

Unsteady convective pressure diffusive source, where (according to Newton's Law of Viscosity),

$$\tau_{xy}=\tau_{yx}=\mu\left(\frac{\partial v}{\partial x}+\frac{\partial u}{\partial y}\right)$$

$$\tau_{xz}=\tau_{zx}=\mu\left(\frac{\partial w}{\partial x}+\frac{\partial u}{\partial z}\right)$$

$$\tau_{yz}=\tau_{zy}=\mu\left(\frac{\partial v}{\partial z}+\frac{\partial w}{\partial y}\right)$$

$$\tau_{xx}=\lambda(\nabla.V)+2\mu\frac{\partial u}{\partial x}\quad,\qquad \tau_{yy}=\lambda(\nabla.V)+2\mu\frac{\partial v}{\partial y},$$

$$\tau_{zz}=\lambda(\nabla.V)+2\mu\frac{\partial w}{\partial z}$$

$$\lambda = -\frac{2}{3}\mu$$

5.4 STOKES HYPOTHESIS:

The Naiver-Stokes equations form the basis upon which the entire science of viscous flow theory has been developed. In general, the continuity and energy equations are also included in the Navier-Stokes equation.

5.5 ENERGY EQUATION:

This equation is based on the principle of conservation of energy, which is generally referred to as the first law of thermodynamics, which states that "energy" can neither created nor destroyed but can only be changed from one form to another form. Energy equation in conservative form is

$$\frac{\partial}{\partial t}\left[\rho\left(e+\frac{V^2}{2}\right)\right]+\nabla\cdot\left[\rho\left(e+\frac{V^2}{2}\right)V\right]=\rho\dot{q}+\frac{\partial}{\partial x}\left(k\frac{\partial T}{\partial x}\right)+\frac{\partial}{\partial y}\left(k\frac{\partial T}{\partial y}\right)+\frac{\partial}{\partial z}\left(k\frac{\partial T}{\partial z}\right)-\frac{\partial(up)}{\partial x}-\frac{\partial(vp)}{\partial y}-\frac{\partial(wp)}{\partial z}$$

$$+\frac{\partial(u\tau_{xx})}{\partial x}+\frac{\partial(u\tau_{yx})}{\partial y}+\frac{\partial(u\tau_{zx})}{\partial z}+\frac{\partial(v\tau_{xy})}{\partial x}+\frac{\partial(v\tau_{yy})}{\partial y}+\frac{\partial(v\tau_{zy})}{\partial z}+\frac{\partial(w\tau_{xz})}{\partial x}+\frac{\partial(w\tau_{yz})}{\partial y}+\frac{\partial(w\tau_{zz})}{\partial z}+pf.V$$

5.6 REYNOLDS AVERAGED NAVIER-STOKES EQUATIONS:

The mean value of a hydrodynamic quantity, for example, the Xi component of the velocity, U_i, is defined by

$$\bar{u}_i=\frac{1}{T}\int_{t_0}^{t_0+T}u_i\,dt$$

In which to be any arbitrary time, and T is the time over which the mean is taken, should be large compared to the period of the random fluctuations associated with turbulence. This is called time averaging.

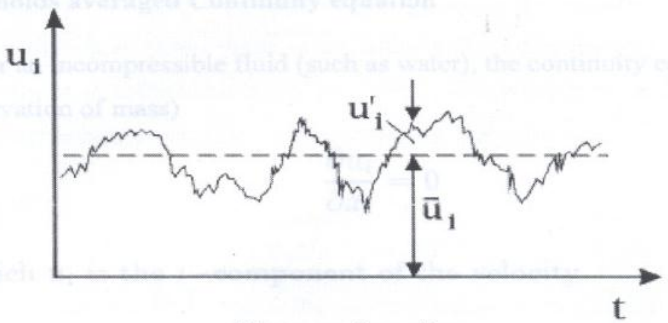

Time series of u_i.

The instantaneous value of the velocity U_i may be written as

$$u_i = \bar{u}_i + u_i'$$

In which u_i' is called the fluctuating part (or fluctuation) of u_i and $\bar{u}_i$ is its mean. This is called the Reynolds decomposition. The Reynolds decomposition can be applied to any hydrodynamic quantity.

5.7 REYNOLDS AVERAGED CONTINUITY EQUATION:

For an incompressible fluid (such as water), the continuity equation is (from the conservation of mass)

$$\frac{\partial u_i}{\partial x_i} = 0$$

In which Ui is the i -component of the velocity.

Averaging gives:

Subtracting the preceding equation gives $\frac{\partial \bar{u}_i}{\partial x_i} = \frac{\partial \bar{u}_i}{\partial x_i} = 0$

equation from continuity

$$\frac{\partial u_i'}{\partial x_i} = 0$$

The above two equations are, the continuity equation for the mean velocity and the continuity equation for its fluctuating part respectively.

5.8 REYNOLDS AVERAGED MOMENTUM EQUATION:

The momentum equation in conservation form is

$$\frac{\partial(\rho u)}{\partial t} + \frac{\partial(\rho u^2)}{\partial x} + \frac{\partial(\rho uv)}{\partial y} + \frac{\partial(\rho uw)}{\partial z} = -\frac{\partial p}{\partial x} + \frac{\partial \tau_{xx}}{\partial x} + \frac{\partial \tau_{yx}}{\partial y} + \frac{\partial \tau_{zx}}{\partial z} + \rho f_x$$

$$\frac{\partial(\rho v)}{\partial t} + \frac{\partial(\rho uv)}{\partial x} + \frac{\partial(\rho v^2)}{\partial y} + \frac{\partial(\rho vw)}{\partial z} = -\frac{\partial p}{\partial y} + \frac{\partial \tau_{xy}}{\partial x} + \frac{\partial \tau_{yy}}{\partial y} + \frac{\partial \tau_{zy}}{\partial z} + \rho f_y$$

$$\frac{\partial(\rho w)}{\partial t} + \frac{\partial(\rho uw)}{\partial x} + \frac{\partial(\rho vw)}{\partial y} + \frac{\partial(\rho w^2)}{\partial z} = -\frac{\partial p}{\partial z} + \frac{\partial \tau_{xz}}{\partial x} + \frac{\partial \tau_{yz}}{\partial y} + \frac{\partial \tau_{zz}}{\partial z} + \rho f_z$$

5.9 UNSTEADY CONVECTIVE PRESSURE DIFFUSIVE SOURCE:

After decomposing the dependent variables in the conservation equations into time-averaged (obtained over an appropriate time interval) and fluctuating components, the equation becomes:

$$\frac{\partial(\rho U)}{\partial t} + div(\rho UU) = -\frac{\partial \rho}{\partial x} + div(\mu grad U) + \left[-\frac{\partial(\rho \overline{u'^2})}{\partial x} - \frac{\partial(\rho \overline{u'v'})}{\partial y} - \frac{\partial(\rho \overline{u'w'})}{\partial z} \right] + S_{Mx}$$

$$\frac{\partial(\rho V)}{\partial t} + div(\rho VU) = -\frac{\partial \rho}{\partial y} + div(\mu grad V) + \left[-\frac{\partial(\rho \overline{u'v'})}{\partial x} - \frac{\partial(\rho \overline{v'^2})}{\partial y} - \frac{\partial(\rho \overline{v'w'})}{\partial z} \right] + S_{My}$$

$$\frac{\partial(\rho W)}{\partial t} + div(\rho WU) = -\frac{\partial \rho}{\partial z} + div(\mu grad W) + \left[-\frac{\partial(\rho \overline{u'w'})}{\partial x} - \frac{\partial(\rho \overline{v'w'})}{\partial y} - \frac{\partial(\rho \overline{w'^2})}{\partial z} \right] + S_{Mz}$$

Comparison of these equations with conservation equations indicates that, in the case of the turbulent flow, there is an additional stress term, $-\rho \overline{u_i' u_j'}$. This additional stress is called the Reynolds stress. There are nine such stresses in the time averaged momentum equations, out of which six are unknowns.

$$-\rho \overline{u_i' u_j'} = \begin{bmatrix} -\rho \overline{u_1' u_1'} & -\rho \overline{u_1' u_2'} & -\rho \overline{u_1' u_3'} \\ -\rho \overline{u_2' u_1'} & -\rho \overline{u_2' u_2'} & -\rho \overline{u_2' u_3'} \\ -\rho \overline{u_3' u_1'} & -\rho \overline{u_3' u_2'} & -\rho \overline{u_3' u_3'} \end{bmatrix}$$

Whereas, there are ten unknowns (namely, three components of the velocity, $\bar{u}_i$, pressure, $\bar{\rho}$ and six components of the Reynolds stress $-\rho \overline{u_i' u_j'}$, hence the system is not closed. This problem is known as the closure problem of turbulence.

Therefore, Reynolds equations cannot be solved directly, because the new apparent turbulent stresses are new unknowns. To proceed further, it is necessary to find additional equations involving the unknowns or make assumptions regarding the relation between the new apparent turbulent quantities and the time-mean variables. This is known as the closure problem, which is handled through turbulence modeling.

5.10 TURBULENCE MODELING:

The RNG k-ε turbulence model:

Transport Equations for the RNG *k*- ω Model

$$\frac{\partial}{\partial t}(\rho k) + \frac{\partial}{\partial x_i}(\rho k u_i) = \frac{\partial}{\partial x_j}\left(\alpha_k \mu_{\text{eff}} \frac{\partial k}{\partial x_j}\right) + G_k + G_b - \rho\epsilon - Y_M +$$

$$\frac{\partial}{\partial t}(\rho\epsilon) + \frac{\partial}{\partial x_i}(\rho\epsilon u_i) = \frac{\partial}{\partial x_j}\left(\alpha_\epsilon \mu_{\text{eff}} \frac{\partial \epsilon}{\partial x_j}\right) + C_{1\epsilon}\frac{\epsilon}{k}(G_k + C_{3\epsilon}G_b) - C_{2\epsilon}\rho\frac{\epsilon^2}{k} - R$$

In these equations,

k= Turbulent kinetic energy

ε = Specific dissipation Rate

The term $\tilde{G}_k$ represents the production of turbulence kinetic energy

The term G_b is the generation of turbulence kinetic energy due to buoyancy

α_k and α_ϵ are the inverse effective Prandtl numbers for k and ϵ

S_k And S_ω are user-defined source terms.

Y_M represents the contribution of the fluctuating dilatation in compressible turbulence to the overall dissipation rate

These k and ω, values are used to compute Reynolds stress tensor.

SIMULATION OF CAR BODY

The geometry of the Mahindra is shown in the figure. This was created in the CATIA software by taking the dimensions of the car body in X, Y and Z directions. After the creation of geometry, it was imported to the Ansys workbench design modeler Figure in which the domain Figure was created around the profile of the car body of a four-wheeler. In this design modeler, scaling has to be given to the profile in order to simulate the experiment using CFD software.

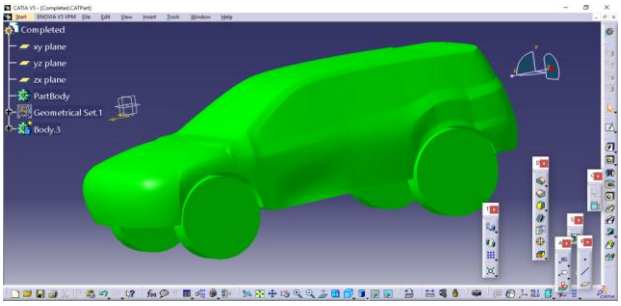

Fig: 6.1 Geometry of Mahindra existing car profile.

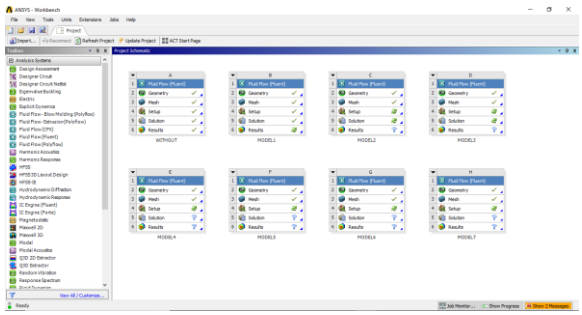

Fig: 6.2 Ansys window layout.

6.1 GEOMETRY IMPORTED TO WORK BENCH DESIGN MODELER:

Mahindra car profile**:**

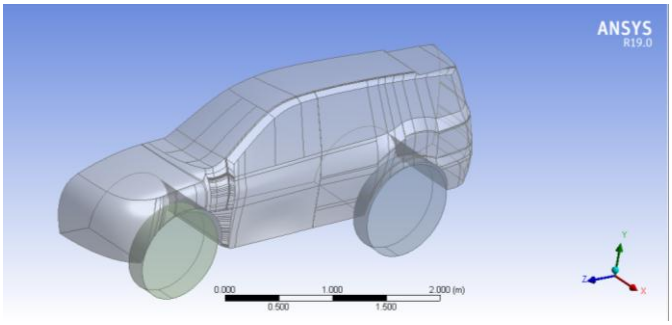

Figure: 6.3 Geometry in Design Modeler

Domain of Mahindra car profile:

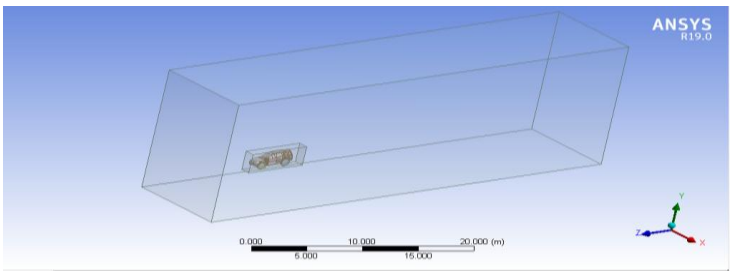

Figure: 6.4 Domain of the Geometry

6.2 MESHING:

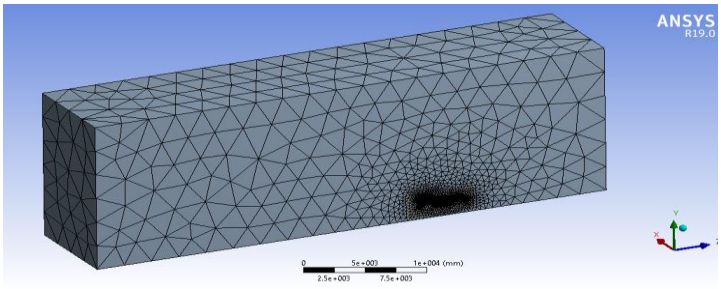

Figure: 6.5 Meshing of car profile

Boundary conditions

Material properties:

Name: Air

Type: Fluid

Density, ρ = 1.255 Kg/m^3

Viscosity, μ = 1.7894*e-5 Kg/m-s

Boundary conditions:

Inlet condition: velocity (80km/hr)

Outlet condition: pressure (0 Pa)

Wall condition: stationary and no slip

Solution methods:

Scheme: SIMPLE (Semi Implicit Method for Pressure Linked Equation)

Gradient: Least Squares Cell Based

Pressure: Standard

Momentum: Second order up wind

Boundaries in CFX-PRE:

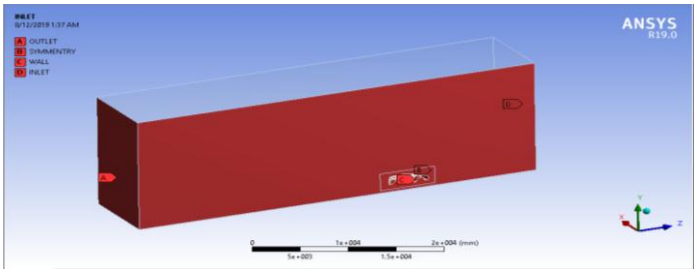

Fig: 6.6 Boundary conditions.

6.5 SOLVER SETTINGS:

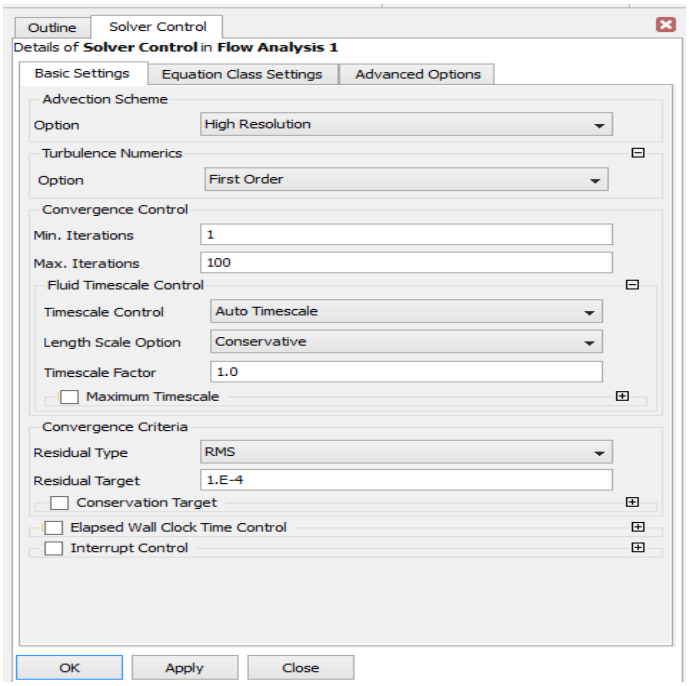

Figure: 6.7 Solver settings

The above figure shows that the solver settings to be given in the solver. In convergence control, the maximum number of iterations given is 50. The residual type is given as RMS.

6.6 RESIDUAL MONITORS:

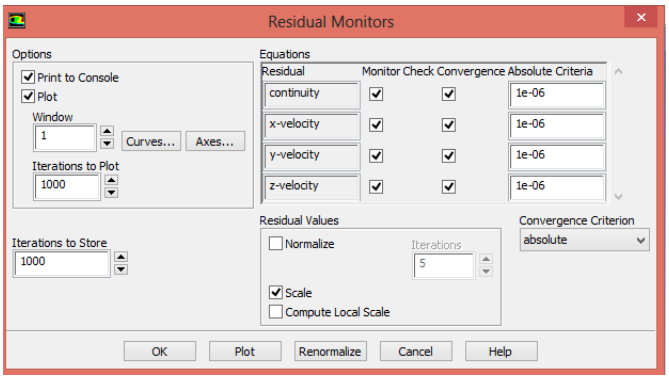

Figure: 6.8 Residual monitors

The above figure shows the residual monitors to be given before the solution run. At the end of each solver iteration, the residual sum for each of the conserved variables is computed and stored, thereby recording the convergence history. This history is also saved in the data file.

Simulation graph in figure shows the variation of variable value with respect to the accumulated time step. The variable value here is the RMS value for continuity

equation and momentum equation (X-mom, Y-mom, and Z-mom)

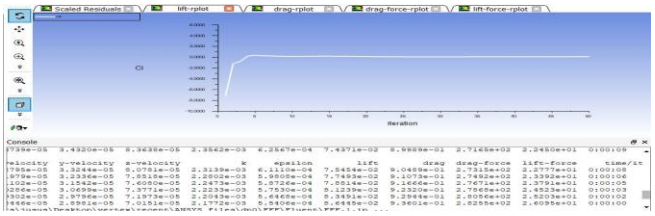

Fig: 6.9 coefficient of lift curve of without VG.

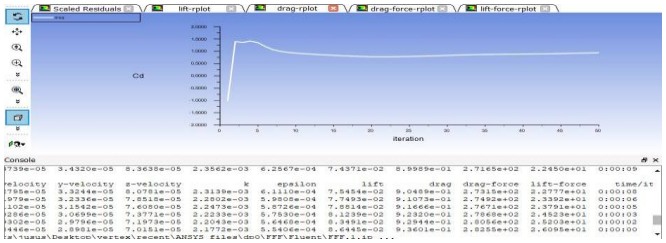

Fig: 6.10 coefficient of Drag curve of without VG.

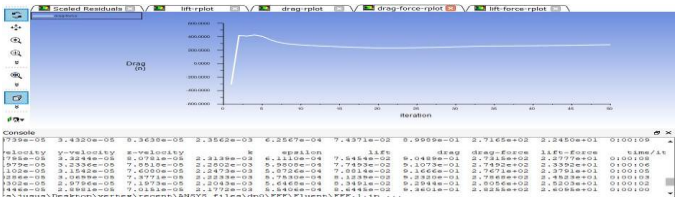

Fig: 6.11 Drag force on car body curve of without VG

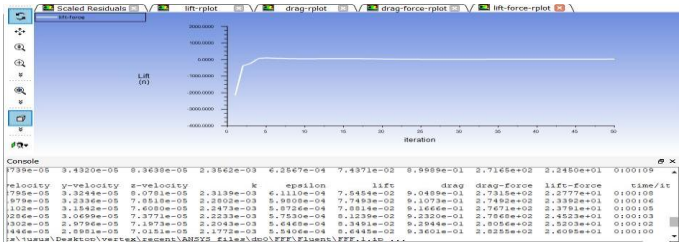

Fig: 6.12 lift force on car body curve of without VG.

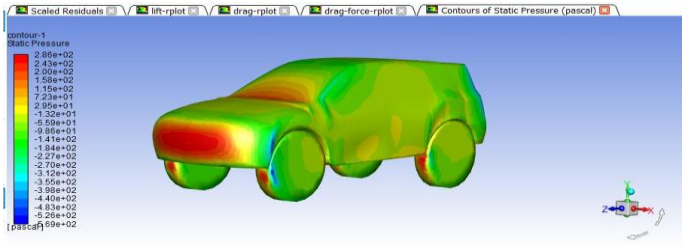

Fig: 6.13 pressure contour on car body without VG

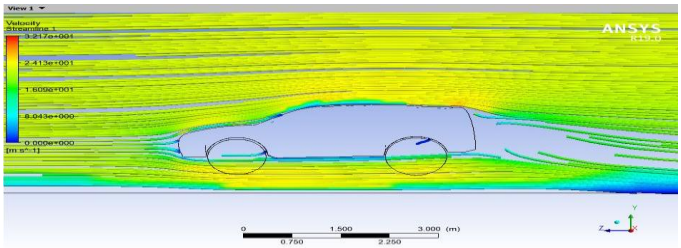

Fig: 6.14 velocity steam line around car body without VG.

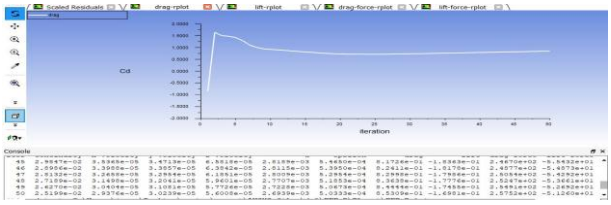

Fig: 6.15 coefficient of Drag curve of model 7.

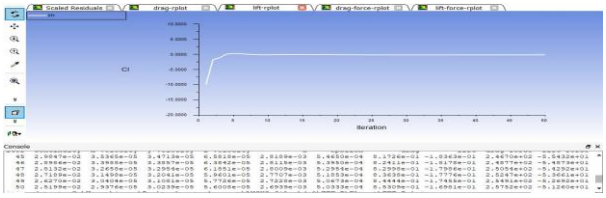

Fig: 6.16 coefficient of lift curve of model 7.

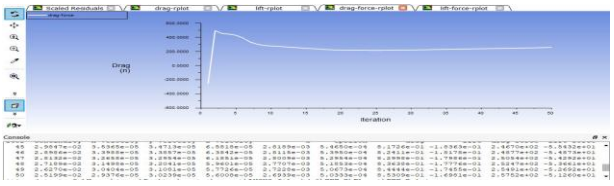

Fig: 6.17 Drag force on car body curve of model 7.

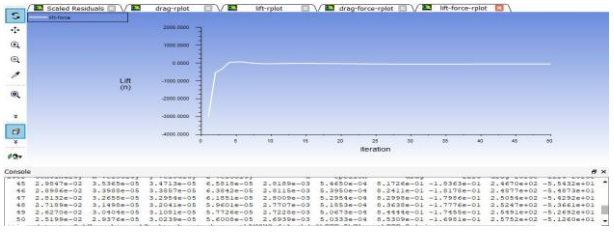

Fig: 6.18 Lift force on car body curve of model 7.

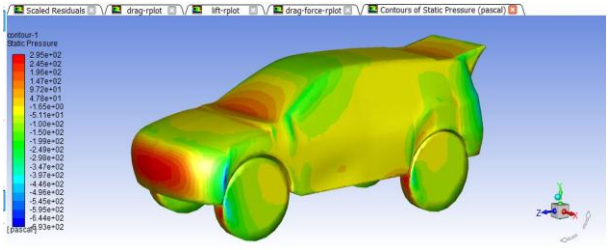

Fig: 6.19 pressure contour on car body model 7.

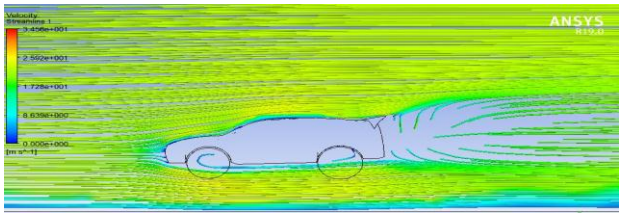

Fig: 6.20 velocity steam line around car body model 7. sss

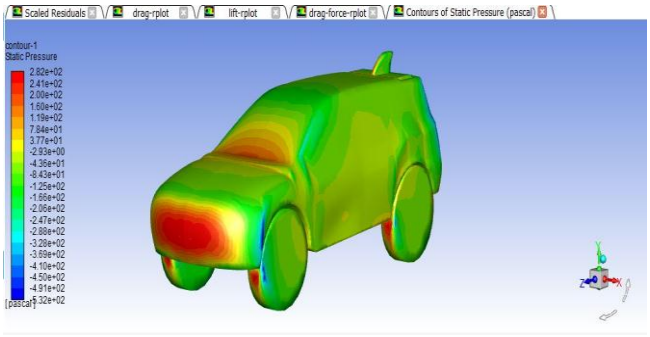

Fig: 6.23 pressure contour on car body model 2.

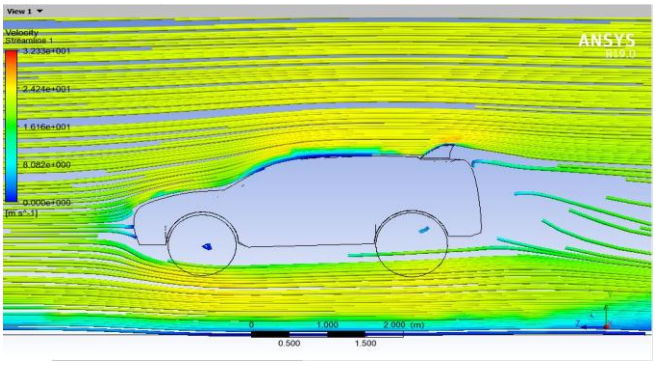

Fig: 6.24 velocity steam line around car body model 2.

RESULTS AND DISCUSSION

Table: 7.1 Drag coefficient of car body.

MODEL NUMBER	DRAG COEFFICIENT
WITHOUT	0.936
MODEL 1	0.927
MODEL 2	0.854
MODEL 3	0.88
MODEL 4	0.902
MODEL 5	0.889
MODEL 6	0.932
MODEL 7	0.853

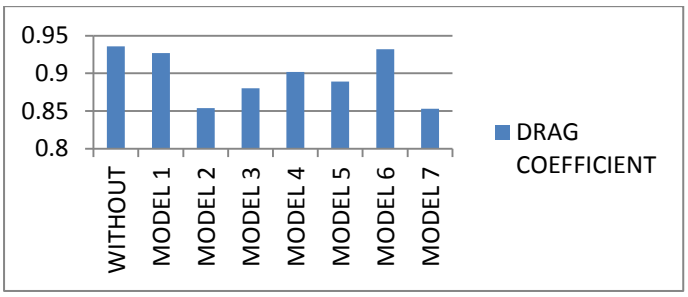

Graph: 7.1Drag coefficient of car body.

Table: 7.2 lift coefficient of car body.

MODEL NUMBER	LIFT COEFFICIENT
WITHOUT	8.60E-02
MODEL 1	4.42E-02
MODEL 2	2.97E-02
MODEL 3	7.40E-02
MODEL 4	6.70E-02
MODEL 5	7.20E-02
MODEL 6	8.17E-02
MODEL 7	1.69E-02

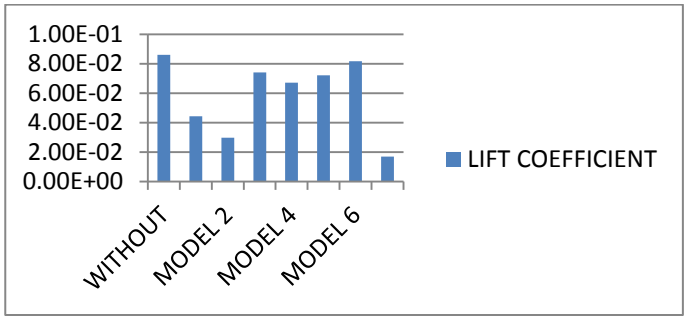

Graph: 7.2 lift coefficient of car body.

Table: 7.3 Drag force acting on car body.

MODEL NUMBER	DRAG FORCE
WITHOUT	2.82E+02
MODEL 1	2.80E+02
MODEL 2	2.58E+02
MODEL 3	2.65E+02
MODEL 4	2.72E+02
MODEL 5	2.68E+02
MODEL 6	2.81E+02
MODEL 7	2.57E+02

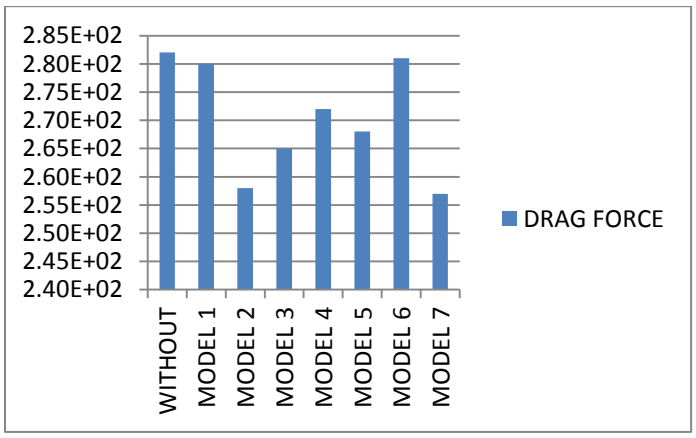

Graph: 7.3 Drag force acting on car body.

Table: 7.4 Lift force acting on car body.

MODEL NUMBER	LIFT FORCE
WITHOUT	2.60E+01
MODEL 1	1.30E+01
MODEL 2	8.90E+00
MODEL 3	2.25E+01
MODEL 4	2.03E+01
MODEL 5	2.17E+01
MODEL 6	2.46E+01
MODEL 7	2.20E+00

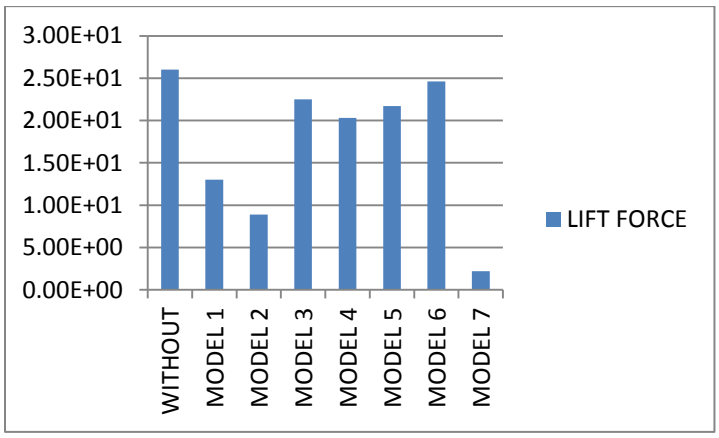

Graph: 7.4 Lift force acting on car body.

Table: 7.5 pressure acting on car body.

MBER	PRESSRE
WITHOUT	2.86E+02
MODEL 1	2.84E+02
MODEL 2	2.82E+02
MODEL 3	2.97E+02
MODEL 4	2.92E+02
MODEL 5	2.87E+02
MODEL 6	2.85E+02
MODEL 7	2.95E+02

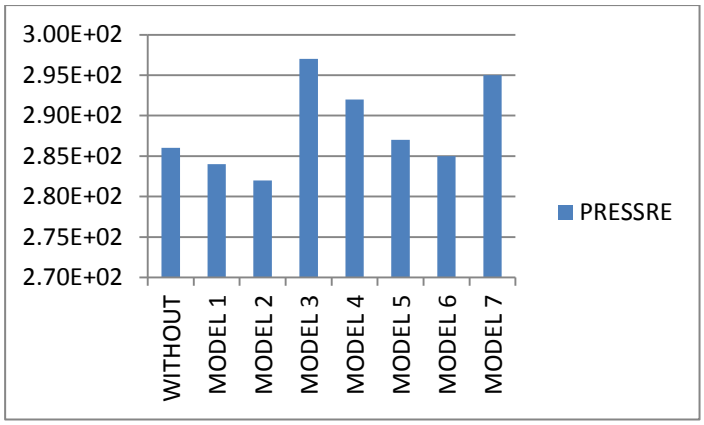

Graph: 7.5 pressure acting on car body.

Table: 7.6 air velocity after cross the car body.

MODEL NUMBER	MAX AIR VELOCITY
WITHOUT	3.21E+01
MODEL 1	3.14E+01
MODEL 2	3.23E+01
MODEL 3	3.32E+01
MODEL 4	3.42E+01
MODEL 5	3.29E+01
MODEL 6	3.39E+01
MODEL 7	3.45E+01

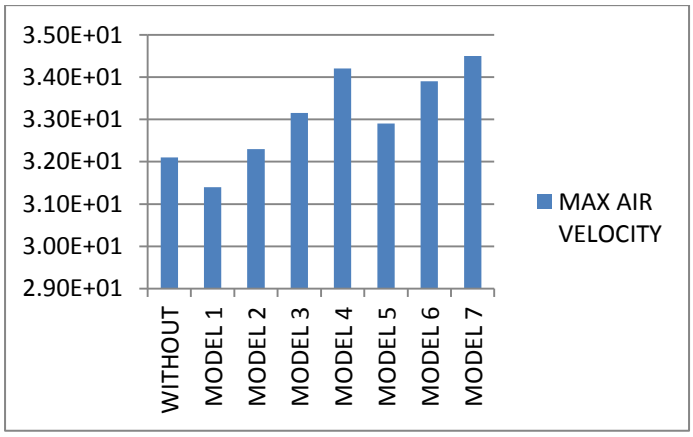

Graph: 7.6 air velocity after cross the car body.

CONCLUSIONS

- By the simulation results on existing and modified car designs with vertex generators, the modified car model 7 has less drag and less average static pressure when compared with that of existing design of Mahindra at a given angle and speed.
- The minimum drag observed after developing the front and rear modifications on car body.
- Thus, our design gets less turbulence leading to the increase in fuel efficiency and vehicle stability.

REFERENCES

1. James Keog, Tracie Barber, Sammy Diasinos, Doig Graham, Aerospace Engineering Department, California Polytechnic State University, School of Mechanical and Manufacturing Engineering, UNSW, Australia-2016.
2. Alamaan Altaf a, Ashraf A. Omar b, Waqar Asrar Department of Aeronautical Engineering, University of Tripoli, P.O. Box 13154, Tripoli-Libya -2014.
3. Sneh Hetawala, Mandar Gophaneb, Ajay B.K.C, Yagna valkya Mukkamalad a, b, c, Second year M.Tech. (Automotive Engineering), School of Mechanical and Building Sciences, VIT University, Vellore, Tamilnadu, India. d Professor, Thermal and Automotive Division, School of Mechanical and Building Sciences, VIT University, Vellore, Tamilnadu, India. 2014.
4. D.E. Aljure a , O. Lehmkuhl a, b , I. Rodríguez a , A. Oliva a, a Heat and Mass Transfer Technological Center (CTTC), Universitat Politecnica de Catalunya-BarcelonaTech (UPC), ETSEIAT, Colom 11, 08222 Terrassa, Barcelona, Spain b Termo Fluids, S.L. Av. Jaquard, 97 1-E, 08222 Terrassa, Barcelona, Spain 2014.
5. CFD modelling of the aerodynamic effect of trees on urban air pollution dispersion J.H. Amorim, V. Rodrigues, R. Tavares, J. Valente, C. Borrego CESAM & Department of Environment and Planning, University of Aveiro, 3810-193 Aveiro, Portugal 2013.
6. S.M. Rakibul Hassan, Toukir Islam, Mohammad Ali, Md. Quamrul Islam Department of Mechanical Engineering, Bangladesh University of Engineering and Technology, Dhaka-1000, Bangladesh 2013.
7. Aerodynamic drag reduction of a simplified square back vehicle using steady blowing R. P. Littlewood M. A. Passmore-2012.
8. S.Y. Cheng a, b,M. Tsubokura , T. Nakashima c ,Y. Okada d , T. Nouzawa Graduate School of Engineering, Hokkaido University, Kita-13,Nishi-8,Kita-ku,Sapporo 060-8628, Japan b Faculty of Mechanical Engineering, University Teknikal Malaysia Melaka, Hang Tuah Jaya, 76100 Durian Tunggal, Melaka, Malaysia c Graduate School of Engineering, Hiroshima University, 1-4-1 Higashi-Hiroshima, Hiroshima 739857, Japan d Vehicle Testing & Research Department, Mazda Motor Corporation, Aki Gun, Hiroshima 7308670, Japan 2012.
9. Computational aero-acoustic analysis of a passenger car with a rear spoiler Chien-Hsiung Tsai a, Lung-Ming Fu b, Chang-Hsien Tai a, Yen-Luong Huang a, Jik-Chang Leong a,* aDepartment of Vehicle Engineering, National Pingtung University of Science and Technology, Pingtung 912, Taiwan department of Material Engineering, National Pingtung University of Science and Technology, Pingtung 912, Taiwan-2009.
10. W. Angelis, D. Drikakis, F. Durst, W. Khier Institute of Fluid Mechanics', University of Erlangen-Nuremberg, Cauerstr. 4, D-91058 Erlangen, September 1996.